

Original Research Article

RESERVOIR STUDY USING PETROPHYSICAL PROPERTIES OF AN OFFSHORE FIELD IN NIGER DELTA BASIN

ABSTRACT

A qualitative and quantitative reservoir study of an offshore field (BAK field), was carried out using the analysis of the petrophysical properties of the reservoirs in the field. Five well were acquired and utilized to carry out this study, from the wells, three reservoir intervals were identified through quantitative interpretation. Reservoir correlation was carried out to identify lithostratigraphic sand unit within the formations of the wells, with the top and base markers distinguishing the reservoirs mapped, the sand bodies of the reservoirs were found to be heterogeneous and continuous. The three reservoir intervals identified were named: BAK_1, BAK_2, and BAK_3 reservoirs respectively, reservoir sedimentology revealed that the reservoirs were predominantly sands with intercalated shale within the formations. The results of petrophysical analysis revealed that the Net-to-Gross (NTG) values within the identified reservoir were 83%, 86%, and 85% for BAK_1, BAK_2, and BAK_3 reservoirs respectively, while the total porosity/effective porosity were found to be 28% / 24% for Bak_1, 27% / 24%, for Bak_2 and 28% / 18% for Bak_3 respectively. The permeability values were 2279.558 mD, 2178.738 mD, and 2760.678 mD while the water saturation was estimated as 45%, 48%, and 48% for BAK_1, BAK_2, and BAK_3 reservoirs respectively. From the results of petrophysical analysis, which reveals a low shale volume, good and effective porosity, high permeability and low average water saturation. The field can be classified as a good candidate for optimum production of hydrocarbon.

Comment [R1]: wells

Comment [R2]: Use period . From

Keywords: Quantitative Analysis, Qualitative, Petrophysical, lithostratigraphic, Heterogeneity, Optimum, Sedimentology.

1. INTRODUCTION

In subsurface characterization, the understanding of the underlying geological formation helps to accurately predict the potentials and to estimate reserves of hydrocarbon in the reservoir of the field. Information extracted from interpreted cores, seismic data and well logs help to further understand the underlying formation of rocks, and this helps to characterize the reservoirs found within these formations. Reservoir is a subsurface rock that has effective porosity and permeability which usually contains commercially exploitable quantity of hydrocarbon [1]. Reservoir rocks of Eocene to Pliocene in age are often stacked, ranges from 15 – 45 meters in thickness [2]. Reservoirs in the Niger Delta exhibit a wide range of complexities in their sedimentological and petrophysical characteristics due to differences in hydrodynamic conditions prevalent during their depositional settings [3]. Petrophysical properties analysis is the quantification, integration, and reduction of all acquired geological data acquired to determine the capability of the reservoir to store and transmit fluids [4]. Petrophysical analysis/evaluation deals with the determination of reservoir properties/parameters such as reservoir thickness, volume of shale (V_{sh}), porosity, either effective or total (Φ), permeability (k), water saturation (S_w), hydrocarbon saturation (S_H), and

net to gross ratio (N/G) [5]. These parameters are very useful and important tools for planning, selecting and implementing important decisions regarding the reservoir development which serves as an integral component in the reservoir characterization workflow [6]. Petrophysical evaluation is also concerned with the rock formation proportion that determines the quality, quantity, recoverability of hydrocarbon in a any given reservoir. It is always essential to integrate petrophysical and engineering data to accurately predict reservoir quality during and after production. Over the last two decades intense petroleum exploration and exploitation activities in the Niger Delta region has led to the accumulation of a vast amount of data making it possible to establish a historical reconstruction and evolution of the Niger Delta basin [7], this study is based on the use of well log data to evaluate the petrophysical properties of the reservoir sand body (reservoir study) in an offshore field in Niger Delta Basin.

1.2. LOCATION OF THE STUDY AREA

The study area is field located within the offshore region of Niger Delta Basin, Nigeria. The field will be referred to as BAK Field, and was discovered by a wildcat, which was further appraised by three other wells based on 2-D seismic data, with the reservoirs of Zanclean of 3rd order sequences, the field was penetrated by five wells, BAK field lies between longitude 7°39'3.17"E and latitude 4°8'19.30"N and is located within the offshore depobel region of the basin (Figure 1).

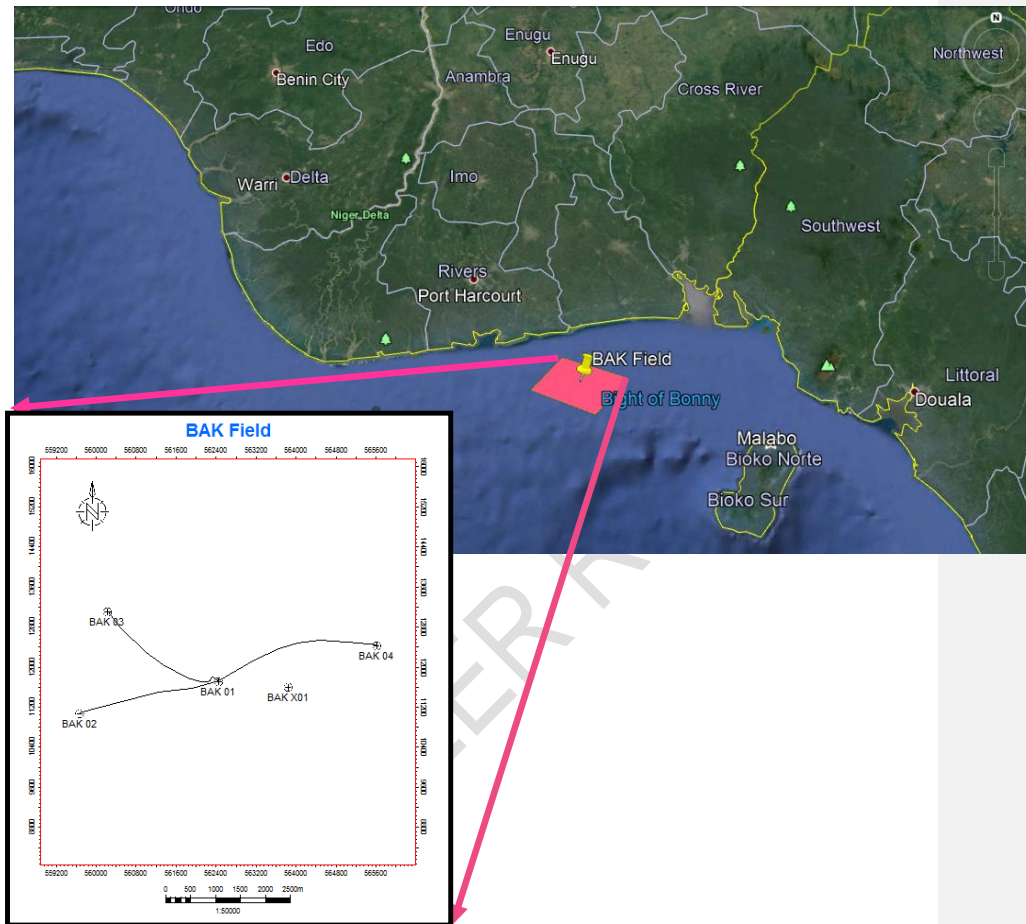


Fig. 1: A map showing the location of the BAK Field, Offshore Niger Delta (Source: Google Earth 2021) and the Base map for BAK Field showing the distribution of wells within the area

1.3. GEOLOGY OF NIGER DELTA

Niger Delta is found within the Gulf of Guinea, increases down towards the Niger Delta Province and varies from the Eocene age to this present time [8]. The delta has prograded southwestward, creating depobelts that constitute the most vital part of the delta at every development stage [9]. The basin is bounded in the north by older (Cretaceous) tectonic elements among which are the Anambra Basin, Abakaliki uplift and Afikpo syncline. Weber [10] suggested that the basin which facilitated and controlled the formation of the present Niger delta was developed by lift faulting during the Precambrian. Benin and Calabar Hinge lines are the deep-seated faults associated with the rifting-controlled formation of the delta. The building of the Niger Delta (Figure 2) over the edge of the African continent began in the

middle-late Eocene [11]. Evidence from geological investigation indicates that the Oligocene and younger sediments progressive toward the continental shelf and they average 26,000 ft (7924 m) [12]. The accumulation of these sediments was rather fast and hence gravitational movements within them became pronounced, resulting in contemporaneous faulting with deposition (growth faults) [13]. According to Orife and Avbovbo [14], the Tertiary Niger Delta extends over an area of approximately 75,000 sq km and consists of a regressive clastic sequence, which attains a topmost thickness of 12,000 m. The Niger Delta is regarded as one of the most prolific oil and gas provinces in the world [15]. Niger delta basin is known to be divided into three large scale lithostratigraphic unit: (1) the basal Paleocene to Recent pro-delta facies of the Akata formation, (2) Eocene to recent, paralic facies of the Agbada Formation, and (3) Oligocene to recent, fluvial facies of the Benin formation and the formation reflect a gross coarsening upward progradational clastic wedge, and deposited in Marine, Deltaic and fluvial environments (Figure 3). The Tertiary Niger Delta is characterized by syndimentary gravitational growth faults developed as a result of a rapid sand deposition and differential loading of coarser clastics over fined grained undercompacted marine shale of the Akata Formation [2, 16, 17, 18]. These discoveries have onshore on the continental shelf, and in deep water. Niger Delta province has a commercial accumulation of oil and gas. The production of oil and gas originates from accumulation in the pore spaces of reservoir rocks usually sandstone, limestone and dolomite. The formation is characterized by altering sandstone and shale units varying in thickness from 100 ft to 1500 ft [2]. The growth faults are contemporaneous and more or less continuously active with deposition such that their throws increase with depth. The growth fault may be listric, typically cusped normal faults, which flatten with depth into the thick clastic shaly sequence of the Akata Formation. The continuous growth of the faults after their inception, allows for greater sedimentation on the down-thrown blocks relative to the up-thrown blocks [2, 9, 17, 18].

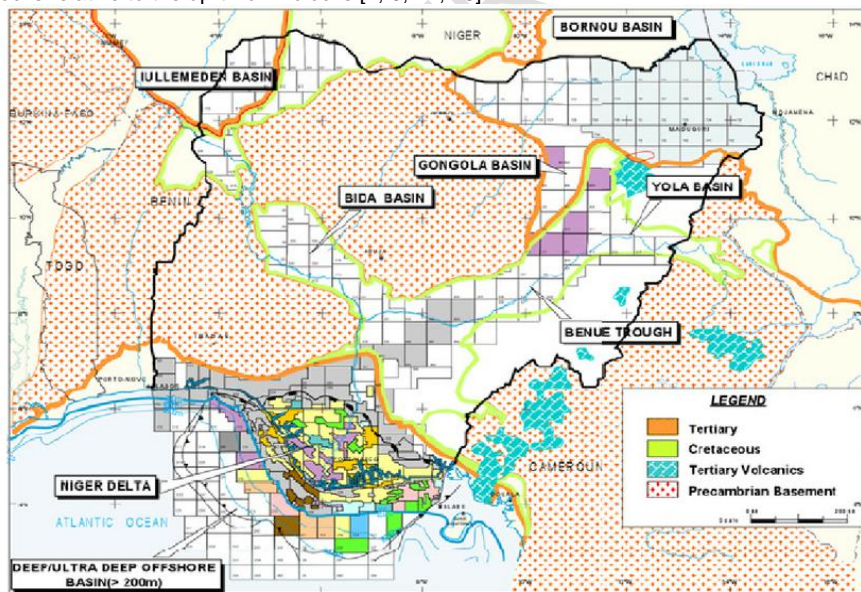


Fig. 2: Map of Nigeria showing Niger Delta Basin Area and its Geological formation (Total Nig. Plc)

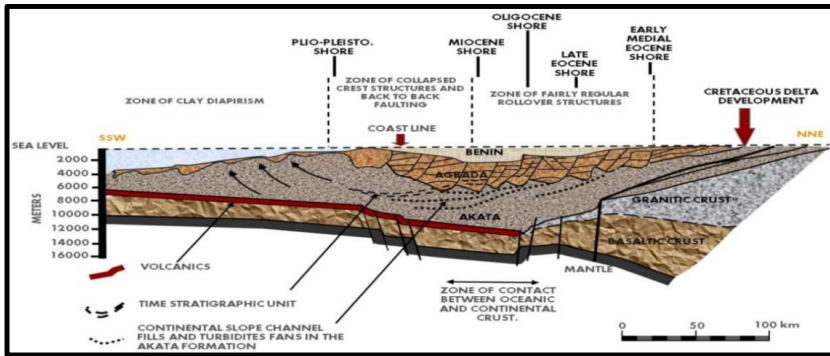


Fig. 3: Schematic dip section of the Niger Delta (Modified from Weber and Daukoru, 1975)

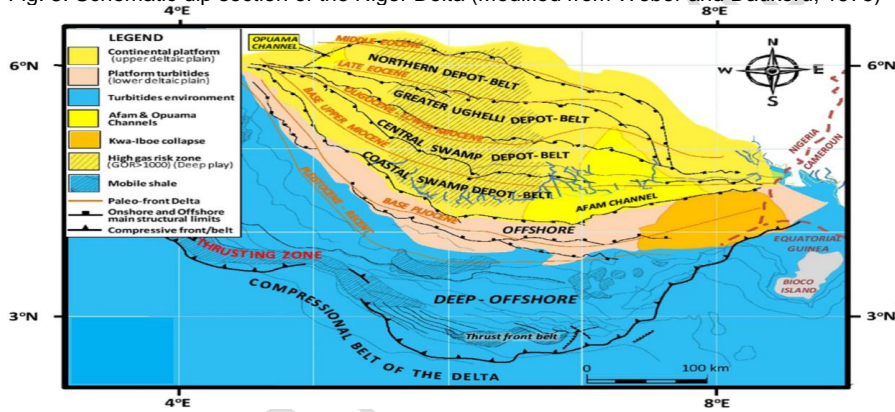


Fig. 4: Sectional map of the Niger Delta depobelts and structural limits (Redrawn from Doust and Omatsola, 1990)

This figure presents the regional stratigraphy of the Western Niger Delta, divided into Offshore and Onshore units. It includes a stratigraphic column on the left with lithofacies units and a depobelt penetration chart on the right.

- Offshore Units:** Akata Group (Basinal & slope, marine shale facies with sporadic lowstand turbidite sands), West Delta Erosive (Transpressive, ophiolites), and IMO Shales (Marine shales).
- Onshore Units:** Benin Group (Continental sands with fluvial & distributary channels), Opuama/Osare Channel (Erosional truncation), and Afam Channel.
- Depobelt Penetration (after Shell):** Offshore, Coastal Swamp, Central Swamp, Greater Ughelli, Northern Delta, and Northern Fringes of the Niger Delta (Anambra Basin).

 The stratigraphic column lists lithofacies units such as P1-P14, P15-P18, P19-P22, P23-P26, P27-P30, P31-P34, P35-P38, P39-P42, P43-P46, P47-P50, P51-P54, P55-P58, P59-P62, P63-P66, P67-P70, P71-P74, P75-P78, P79-P82, P83-P86, P87-P90, P91-P94, P95-P98, P99-P102, P103-P106, P107-P110, P111-P114, P115-P118, P119-P122, P123-P126, P127-P130, P131-P134, P135-P138, P139-P142, P143-P146, P147-P150, P151-P154, P155-P158, P159-P162, P163-P166, P167-P170, P171-P174, P175-P178, P179-P182, P183-P186, P187-P190, P191-P194, P195-P198, P199-P202, P203-P206, P207-P210, P211-P214, P215-P218, P219-P222, P223-P226, P227-P230, P231-P234, P235-P238, P239-P242, P243-P246, P247-P250, P251-P254, P255-P258, P259-P262, P263-P266, P267-P270, P271-P274, P275-P278, P279-P282, P283-P286, P287-P290, P291-P294, P295-P298, P299-P302, P303-P306, P307-P310, P311-P314, P315-P318, P319-P322, P323-P326, P327-P330, P331-P334, P335-P338, P339-P342, P343-P346, P347-P350, P351-P354, P355-P358, P359-P362, P363-P366, P367-P370, P371-P374, P375-P378, P379-P382, P383-P386, P387-P390, P391-P394, P395-P398, P399-P402, P403-P406, P407-P410, P411-P414, P415-P418, P419-P422, P423-P426, P427-P430, P431-P434, P435-P438, P439-P442, P443-P446, P447-P450, P451-P454, P455-P458, P459-P462, P463-P466, P467-P470, P471-P474, P475-P478, P479-P482, P483-P486, P487-P490, P491-P494, P495-P498, P499-P502, P503-P506, P507-P510, P511-P514, P515-P518, P519-P522, P523-P526, P527-P530, P531-P534, P535-P538, P539-P542, P543-P546, P547-P550, P551-P554, P555-P558, P559-P562, P563-P566, P567-P570, P571-P574, P575-P578, P579-P582, P583-P586, P587-P590, P591-P594, P595-P598, P599-P602, P603-P606, P607-P610, P611-P614, P615-P618, P619-P622, P623-P626, P627-P630, P631-P634, P635-P638, P639-P642, P643-P646, P647-P650, P651-P654, P655-P658, P659-P662, P663-P666, P667-P670, P671-P674, P675-P678, P679-P682, P683-P686, P687-P690, P691-P694, P695-P698, P699-P702, P703-P706, P707-P710, P711-P714, P715-P718, P719-P722, P723-P726, P727-P730, P731-P734, P735-P738, P739-P742, P743-P746, P747-P750, P751-P754, P755-P758, P759-P762, P763-P766, P767-P770, P771-P774, P775-P778, P779-P782, P783-P786, P787-P790, P791-P794, P795-P798, P799-P802, P803-P806, P807-P810, P811-P814, P815-P818, P819-P822, P823-P826, P827-P830, P831-P834, P835-P838, P839-P842, P843-P846, P847-P850, P851-P854, P855-P858, P859-P862, P863-P866, P867-P870, P871-P874, P875-P878, P879-P882, P883-P886, P887-P890, P891-P894, P895-P898, P899-P902, P903-P906, P907-P910, P911-P914, P915-P918, P919-P922, P923-P926, P927-P930, P931-P934, P935-P938, P939-P942, P943-P946, P947-P950, P951-P954, P955-P958, P959-P962, P963-P966, P967-P970, P971-P974, P975-P978, P979-P982, P983-P986, P987-P990, P991-P994, P995-P998, P999-P1002, P1003-P1006, P1007-P1010, P1011-P1014, P1015-P1018, P1019-P1022, P1023-P1026, P1027-P1030, P1031-P1034, P1035-P1038, P1039-P1042, P1043-P1046, P1047-P1050, P1051-P1054, P1055-P1058, P1059-P1062, P1063-P1066, P1067-P1070, P1071-P1074, P1075-P1078, P1079-P1082, P1083-P1086, P1087-P1090, P1091-P1094, P1095-P1098, P1099-P1102, P1103-P1106, P1107-P1110, P1111-P1114, P1115-P1118, P1119-P1122, P1123-P1126, P1127-P1130, P1131-P1134, P1135-P1138, P1139-P1142, P1143-P1146, P1147-P1150, P1151-P1154, P1155-P1158, P1159-P1162, P1163-P1166, P1167-P1170, P1171-P1174, P1175-P1178, P1179-P1182, P1183-P1186, P1187-P1190, P1191-P1194, P1195-P1198, P1199-P1202, P1203-P1206, P1207-P1210, P1211-P1214, P1215-P1218, P1219-P1222, P1223-P1226, P1227-P1230, P1231-P1234, P1235-P1238, P1239-P1242, P1243-P1246, P1247-P1250, P1251-P1254, P1255-P1258, P1259-P1262, P1263-P1266, P1267-P1270, P1271-P1274, P1275-P1278, P1279-P1282, P1283-P1286, P1287-P1290, P1291-P1294, P1295-P1298, P1299-P1302, P1303-P1306, P1307-P1310, P1311-P1314, P1315-P1318, P1319-P1322, P1323-P1326, P1327-P1330, P1331-P1334, P1335-P1338, P1339-P1342, P1343-P1346, P1347-P1350, P1351-P1354, P1355-P1358, P1359-P1362, P1363-P1366, P1367-P1370, P1371-P1374, P1375-P1378, P1379-P1382, P1383-P1386, P1387-P1390, P1391-P1394, P1395-P1398, P1399-P1402, P1403-P1406, P1407-P1410, P1411-P1414, P1415-P1418, P1419-P1422, P1423-P1426, P1427-P1430, P1431-P1434, P1435-P1438, P1439-P1442, P1443-P1446, P1447-P1450, P1451-P1454, P1455-P1458, P1459-P1462, P1463-P1466, P1467-P1470, P1471-P1474, P1475-P1478, P1479-P1482, P1483-P1486, P1487-P1490, P1491-P1494, P1495-P1498, P1499-P1502, P1503-P1506, P1507-P1510, P1511-P1514, P1515-P1518, P1519-P1522, P1523-P1526, P1527-P1530, P1531-P1534, P1535-P1538, P1539-P1542, P1543-P1546, P1547-P1550, P1551-P1554, P1555-P1558, P1559-P1562, P1563-P1566, P1567-P1570, P1571-P1574, P1575-P1578, P1579-P1582, P1583-P1586, P1587-P1590, P1591-P1594, P1595-P1598, P1599-P1602, P1603-P1606, P1607-P1610, P1611-P1614, P1615-P1618, P1619-P1622, P1623-P1626, P1627-P1630, P1631-P1634, P1635-P1638, P1639-P1642, P1643-P1646, P1647-P1650, P1651-P1654, P1655-P1658, P1659-P1662, P1663-P1666, P1667-P1670, P1671-P1674, P1675-P1678, P1679-P1682, P1683-P1686, P1687-P1690, P1691-P1694, P1695-P1698, P1699-P1702, P1703-P1706, P1707-P1710, P1711-P1714, P1715-P1718, P1719-P1722, P1723-P1726, P1727-P1730, P1731-P1734, P1735-P1738, P1739-P1742, P1743-P1746, P1747-P1750, P1751-P1754, P1755-P1758, P1759-P1762, P1763-P1766, P1767-P1770, P1771-P1774, P1775-P1778, P1779-P1782, P1783-P1786, P1787-P1790, P1791-P1794, P1795-P1798, P1799-P1802, P1803-P1806, P1807-P1810, P1811-P1814, P1815-P1818, P1819-P1822, P1823-P1826, P1827-P1830, P1831-P1834, P1835-P1838, P1839-P1842, P1843-P1846, P1847-P1850, P1851-P1854, P1855-P1858, P1859-P1862, P1863-P1866, P1867-P1870, P1871-P1874, P1875-P1878, P1879-P1882, P1883-P1886, P1887-P1890, P1891-P1894, P1895-P1898, P1899-P1902, P1903-P1906, P1907-P1910, P1911-P1914, P1915-P1918, P1919-P1922, P1923-P1926, P1927-P1930, P1931-P1934, P1935-P1938, P1939-P1942, P1943-P1946, P1947-P1950, P1951-P1954, P1955-P1958, P1959-P1962, P1963-P1966, P1967-P1970, P1971-P1974, P1975-P1978, P1979-P1982, P1983-P1986, P1987-P1990, P1991-P1994, P1995-P1998, P1999-P2002, P2003-P2006, P2007-P2010, P2011-P2014, P2015-P2018, P2019-P2022, P2023-P2026, P2027-P2030, P2031-P2034, P2035-P2038, P2039-P2042, P2043-P2046, P2047-P2050, P2051-P2054, P2055-P2058, P2059-P2062, P2063-P2066, P2067-P2070, P2071-P2074, P2075-P2078, P2079-P2082, P2083-P2086, P2087-P2090, P2091-P2094, P2095-P2098, P2099-P2102, P2103-P2106, P2107-P2110, P2111-P2114, P2115-P2118, P2119-P2122, P2123-P2126, P2127-P2130, P2131-P2134, P2135-P2138, P2139-P2142, P2143-P2146, P2147-P2150, P2151-P2154, P2155-P2158, P2159-P2162, P2163-P2166, P2167-P2170, P2171-P2174, P2175-P2178, P2179-P2182, P2183-P2186, P2187-P2190, P2191-P2194, P2195-P2198, P2199-P2202, P2203-P2206, P2207-P2210, P2211-P2214, P2215-P2218, P2219-P2222, P2223-P2226, P2227-P2230, P2231-P2234, P2235-P2238, P2239-P2242, P2243-P2246, P2247-P2250, P2251-P2254, P2255-P2258, P2259-P2262, P2263-P2266, P2267-P2270, P2271-P2274, P2275-P2278, P2279-P2282, P2283-P2286, P2287-P2290, P2291-P2294, P2295-P2298, P2299-P2302, P2303-P2306, P2307-P2310, P2311-P2314, P2315-P2318, P2319-P2322, P2323-P2326, P2327-P2330, P2331-P2334, P2335-P2338, P2339-P2342, P2343-P2346, P2347-P2350, P2351-P2354, P2355-P2358, P2359-P2362, P2363-P2366, P2367-P2370, P2371-P2374, P2375-P2378, P2379-P2382, P2383-P2386, P2387-P2390, P2391-P2394, P2395-P2398, P2399-P2402, P2403-P2406, P2407-P2410, P2411-P2414, P2415-P2418, P2419-P2422, P2423-P2426, P2427-P2430, P2431-P2434, P2435-P2438, P2439-P2442, P2443-P2446, P2447-P2450, P2451-P2454, P2455-P2458, P2459-P2462, P2463-P2466, P2467-P2470, P2471-P2474, P2475-P2478, P2479-P2482, P2483-P2486, P2487-P2490, P2491-P2494, P2495-P2498, P2499-P2502, P2503-P2506, P2507-P2510, P2511-P2514, P2515-P2518, P2519-P2522, P2523-P2526, P2527-P2530, P2531-P2534, P2535-P2538, P2539-P2542, P2543-P2546, P2547-P2550, P2551-P2554, P2555-P2558, P2559-P2562, P2563-P2566, P2567-P2570, P2571-P2574, P2575-P2578, P2579-P2582, P2583-P2586, P2587-P2590, P2591-P2594, P2595-P2598, P2599-P2602, P2603-P2606, P2607-P2610, P2611-P2614, P2615-P2618, P2619-P2622, P2623-P2626, P2627-P2630, P2631-P2634, P2635-P2638, P2639-P2642, P2643-P2646, P2647-P2650, P2651-P2654, P2655-P2658, P2659-P2662, P2663-P2666, P2667-P2670, P2671-P2674, P2675-P2678, P2679-P2682, P2683-P2686, P2687-P2690, P2691-P2694, P2695-P2698, P2699-P2702, P2703-P2706, P2707-P2710, P2711-P2714, P2715-P2718, P2719-P2722, P2723-P2726, P2727-P2730, P2731-P2734, P2735-P2738, P2739-P2742, P2743-P2746, P2747-P2750, P2751-P2754, P2755-P2758, P2759-P2762, P2763-P2766, P2767-P2770, P2771-P2774, P2775-P2778, P2779-P2782, P2783-P2786, P2787-P2790, P2791-P2794, P2795-P2798, P2799-P2802, P2803-P2806, P2807-P2810, P2811-P2814, P2815-P2818, P2819-P2822, P2823-P2826, P2827-P2830, P2831-P2834, P2835-P2838, P2839-P2842, P2843-P2846, P2847-P2850, P2851-P2854, P2855-P2858, P2859-P2862, P2863-P2866, P2867-P2870, P2871-P2874, P2875-P2878, P2879-P2882, P2883-P2886, P2887-P2890, P2891-P2894, P2895-P2898, P2899-P2902, P2903-P2906, P2907-P2910, P2911-P2914, P2915-P2918, P2919-P2922, P2923-P2926, P2927-P2930, P2931-P2934, P2935-P2938, P2939-P2942, P2943-P2946, P2947-P2950, P2951-P2954, P2955-P2958, P2959-P2962, P2963-P2966, P2967-P2970, P2971-P2974, P2975-P2978, P2979-P2982, P2983-P2986, P2987-P2990, P2991-P2994, P2995-P2998, P2999-P3002, P3003-P3006, P3007-P3010, P3011-P3014, P3015-P3018, P3019-P3022, P3023-P3026, P3027-P3030, P3031-P3034, P3035-P3038, P3039-P3042, P3043-P3046, P3047-P3050, P3051-P3054, P3055-P3058, P3059-P3062, P3063-P3066, P3067-P3070, P3071-P3074, P3075-P3078, P3079-P3082, P3083-P3086, P3087-P3090, P3091-P3094, P3095-P3098, P3099-P3102, P3103-P3106, P3107-P3110, P3111-P3114, P3115-P3118, P3119-P3122, P3123-P3126, P3127-P3130, P3131-P3134, P3135-P3138, P3139-P3142, P3143-P3146, P3147-P3150, P3151-P3154, P3155-P3158, P3159-P3162, P3163-P3166, P3167-P3170, P3171-P3174, P3175-P3178, P3179-P3182, P3183-P3186, P3187-P3190, P3191-P3194, P3195-P3198, P3199-P3202, P3203-P3206, P3207-P3210, P3211-P3214, P3215-P3218, P3219-P3222, P3223-P3226, P3227-P3230, P3231-P3234, P3235-P3238, P3239-P3242, P3243-P3246, P3247-P3250, P3251-P3254, P3255-P3258, P3259-P3262, P3263-P3266, P3267-P3270, P3271-P3274, P3275-P3278, P3279-P3282, P3283-P3286, P3287-P3290, P3291-P3294, P3295-P3298, P3299-P3302, P3303-P3306, P3307-P3310, P3311-P3314, P3315-P3318, P3319-P3322, P3323-P3326, P3327-P3330, P3331-P3334, P3335-P3338, P3339-P3342, P3343-P3346, P3347-P3350, P3351-P3354, P3355-P3358, P3359-P3362, P3363-P3366, P3367-P3370, P3371-P3374, P3375-P3378, P3379-P3382, P3383-P3386, P3387-P3390, P3391-P3394, P3395-P3398, P3399-P3402, P3403-P3406, P3407-P3410, P3411-P3414, P3415-P3418, P3419-P3422, P3423-P3426, P3427-P3430, P3431-P3434, P3435-P3438, P3439-P3442, P3443-P3446, P3447-P3450, P3451-P3454, P3455-P3458, P3459-P3462, P3463-P3466, P3467-P3470, P3471-P3474, P3475-P3478, P3479-P3482, P3483-P3486, P3487-P3490, P3491-P3494, P3495-P3498, P3499-P3502, P3503-P3506, P3507-P3510, P3511-P3514, P3515-P3518, P3519-P3522, P3523-P3526, P3527-P3530, P3531-P3534, P3535-P3538, P3539-P3542, P3543-P3546, P3547-P3550, P3551-P3554, P3555-P3558, P3559-P3562, P3563-P3566, P3567-P3570, P3571-P3574, P3575-P3578, P3579-P3582, P3583-P3586, P3587-P3590, P3591-P3594, P3595-P3598, P3599-P3602, P3603-P3606, P3607-P3610, P3611-P3614, P3615-P3618, P3619-P3622, P3623-P3626, P3627-P3630, P3631-P3634, P3635-P3638, P3639-P3642, P3643-P3646, P3647-P3650, P3651-P3654, P3655-P3658, P3659-P3662, P3663-P3666, P3667-P3670, P3671-P3674, P3675-P3678, P3679-P3682, P3683-P3686, P3687-P3690, P3691-P3694, P3695-P3698, P3699-P3702, P3703-P3706, P3707-P3710, P3711-P3714, P3715-P3718, P3719-P3722, P3723-P3726, P3727-P3730, P3731-P3734, P3735-P3738, P3739-P3742, P3743-P3746, P3747-P3750, P3751-P3754, P3755-P3758, P3759-P3762, P3763-P3766, P3767-P3770, P3771-P3774, P3775-P3778, P3779-P3782, P3783-P3786, P3787-P3790, P3791-P3794, P3795-P3798, P3799-P3802, P3803-P3806, P3807-P3810, P3811-P3814, P3815-P3818, P3819-P3822, P3823-P3826, P3827-P3830, P3831-P3834, P3835-P3838, P3839-P3842, P3843-P3846, P3847-P3850, P3851-P3854, P3855-P3858, P3859-P3862, P3863-P3866, P3867-P3870, P3871-P3874, P3875-P3878, P3879-P3882, P3883-P3886, P3887-P3890, P3891-P3894, P3895-P3898, P3899-P3902, P3903-P3906, P3907-P3910, P3911-P3914, P3915-P3918, P3919-P3922, P3923-P3926, P3927-P3930, P3931-P3934, P3935-P3938, P3939-P3942, P3943-P3946, P3947-P3950, P3951-P3954, P3955-P3958, P3959-P3962, P3963-P3966, P3967-P3970, P3971-P3974, P3975-P3978, P3979-P3982, P3983-P3986, P3987-P3990, P3991-P3994, P3995-P3998, P3999-P4002, P4003-P4006, P4007-P4010, P4011-P4014, P4015-P4018, P4019-P4022, P4023-P4026, P4027-P4030, P4031-P4034, P4035-P4038, P4039-P4042, P4043-P4046, P4047-P4050, P4051-P4054, P4055-P4058, P4059-P4062, P4063-P4066, P4067-P4070, P4071-P4074, P4075-P4078, P4079-P4082, P4083-P4086, P4087-P4090, P4091-P4094, P4095-P4098, P4099-P4102, P4103-P4106, P4107-P4110, P4111-P4114, P4115-P4118, P4119-P4122, P4123-P4126, P4127-P4130, P4131-P4134, P4135-P4138, P4139-P4142, P4143-P4146, P4147-P4150, P4151-P4154, P4155-P4158, P4159-P4162, P4163-P4166, P4167-P4170, P4171-P4174, P4175-P4178, P4179-P4182, P4183-P4186, P4187-P4190, P4191-P4194, P4195-P4198, P4199-P4202, P4203-P4206, P4207-P4210, P4211-P4214, P4215-P4218, P4219-P4222, P4223-P4226, P4227-P4230, P4231-P4234, P4235-P4238, P4239-P4242, P4243-P4246, P4247-P4250, P4251-P4254, P4255-P4258, P4259-P4262, P4263-P4266, P4267-P4270, P4271-P4274, P4275-P4278, P4279-P4282, P4283-P4286, P4287-P4290, P4291-P4294, P4295-P4298, P4299-P4302, P4303-P4306, P4307-P4310, P4311-P4314, P4315-P4318, P4319-P4322, P4323-P4326, P4327-P4330, P4331-P4334, P4335-P4338, P4339-P4

1.4. NIGER DELTA PETROLUUM SYSTEM

Comment [R3]: Petroleum

Petroleum(hydrocarbons) compounds are carbon formed as a result of the breakdown of organic matter deposited alongside sediments in a reducing environment, from its original state to kerogen and then to hydrocarbon under the right temperature, pressure, and chemical conditions. In the northwestern portion of the delta, the oil window (active source rock interval) lies in the upper Akata Formation and the lower Agbada Formation. To the southeast, the top of the oil window is Stratigraphically lower (up to 4000 below the upper Akata/lower Agbada sequence [2]. The attributed the distribution of the top of the oil window is attributed to the thickness and sand/shale ratios of the overburden rock (Benin formation and variable proportions of the Agbada formation) [9, 19, 20]. The sandy continental sediment (Benin formation) has the lowest thermal gradient (1.3 to 1/8°C/100 m); the paralic Agbada Formation has an intermediate gradient (2.7°C/100 m); and the marine, overpressured Akata Formation has the highest (5.5°C/100 m) [21]. Therefore, within any depobelt, the depth to any temperature is dependent on the gross distribution of sand and shale. If sand/shale ratios were the only variable, the distal offshore subsurface temperatures would be elevated because sand percentages are lower. To the contrary, the depth of the hydrocarbon kitchen is expected to be deeper than in the delta proper, because the depth of oil generation is a combination of factors: temperature, time, and deformation related to tectonic effects [22]. The generation and migration processes occurred sequentially in each depobelts and only after the entire belt was structurally deformed, implying that deformation in the Northern Belt would have been completed in the Late Eocene [2]. The Akata/Agbada formational boundary in this region is currently at a depth of about 4,300 m, with the upper Akata Formation in the wet gas/condensation generating zone (vitrinite reflectance value >1.2); [2, 23]. The lowermost part of the Agbada Formation here entered the oil window sometime in the Late Oligocene.

2.0. MATERIAL AND METHODS

2.1. MATERIALS

This study was carried out using well log data which was acquired from BAK field, shallow offshore Niger Delta. Available data in the well log suite includes Gamma ray (GR) log, Caliper log, Neutron log, Density log, Sonic log and Resistivity (shallow and deep) logs (Table 1) with their well header information and well survey deviation data.

Software

Two main softwares were used for the analysis and interpretation namely:

- **Schlumberger PETREL™ (2017 version) Software:** Used for loading well log data, data appraisal, well correlation, and petrophysical data analysis.
- **Microsoft Excel:** This software will be used for analyzing the result estimated for the petrophysical properties.

2.2. METHODS

Research Workflow

The outlined procedures were utilized for the successful completion of this project; they include the following data sourcing, data gathering, and data loading into relevant software, data quality assurance and quality control, well logs conditioning (despiking and interpolation), well correlation, petrophysical evaluation of reservoirs, visualization and analysis of estimated petrophysical properties.

3. RESULTS AND DISCUSSION

3.1 RESULTS

The results from lithostratigraphic correction revealed that the gamma ray logs depicted two lithologies from top to bottom in the five wells (BAK 01, BAK 02, BAK 03, BAK 04 and BAK X01). The lithologies identified majorly were sands and shales. A total of three reservoir units (BAK_1, BAK_2 and BAK_3) were identified and correlated across all the wells (Fig. 7). These reservoirs were bounded by layers of shale which served as both seals and source rocks. All three reservoirs had intercalated shales at various sections, indicating that the reservoir sands identified are shaly in nature. Petrophysical properties which include shale volume, water saturation, hydrocarbon saturation, permeability, net-to-gross, effective and total porosities were estimated for each of the wells as shown in Figures 8-12, with the estimated values tabulated in Table 2 and Table 3 respectively. The analysis of the petrophysical properties using statistical techniques of correlating their effects during the study, analyses and interpretation of the reservoir was employed using the logs and bar charts as shown in Figures 14 – 21. A plot of the fluid saturation is shown in Figure 22, while the result of the correlation of the STOOIP and permeability is shown in Figure 23.

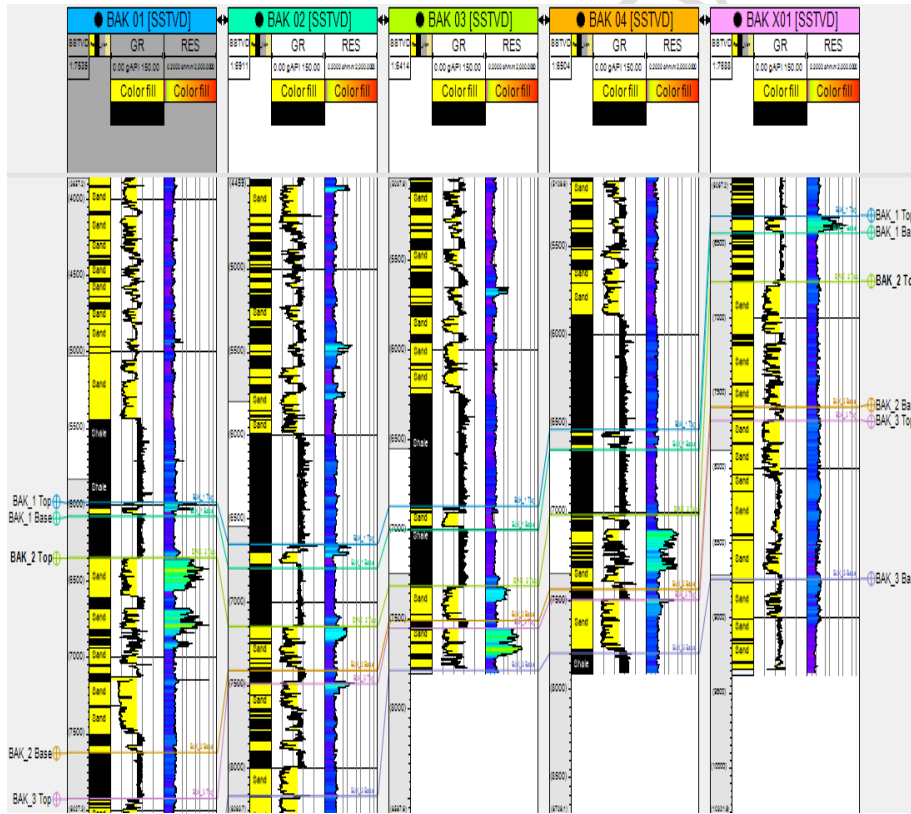


Fig. 7: Lithostratigraphic Correlation of the Five wells in BAK field showing three reservoirs sand units.

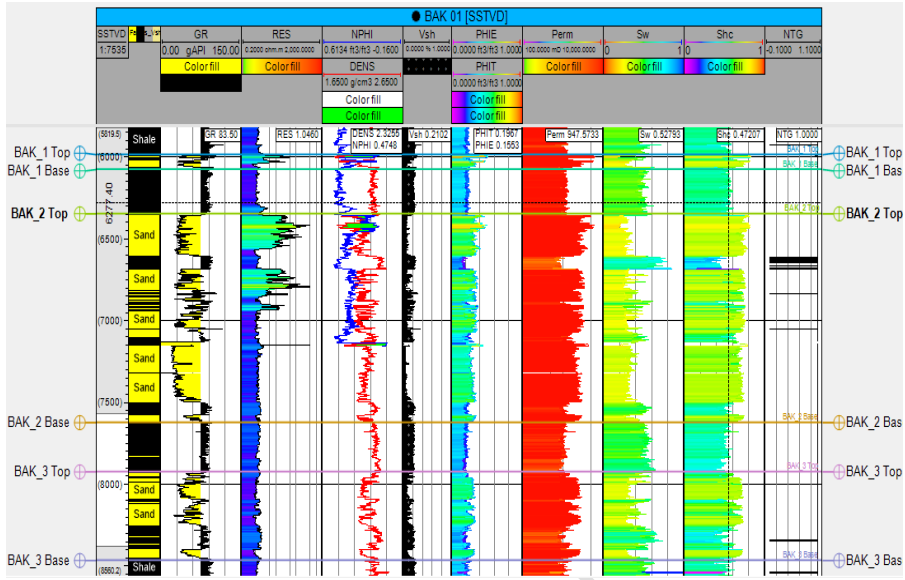


Fig. 8: Well BAK 01 showing correlated Petrophysical parameters

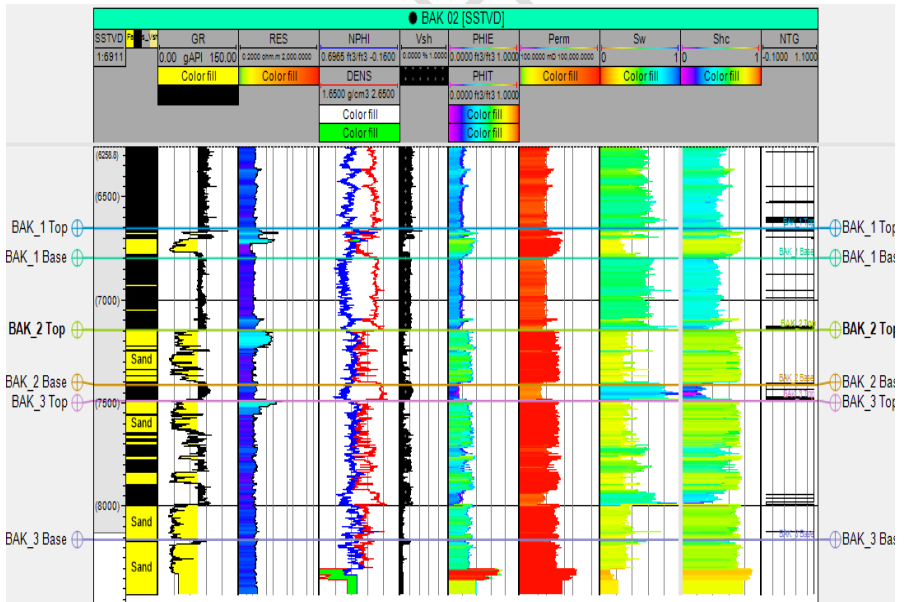


Fig. 9: Well BAK 02 showing correlated Petrophysical parameters

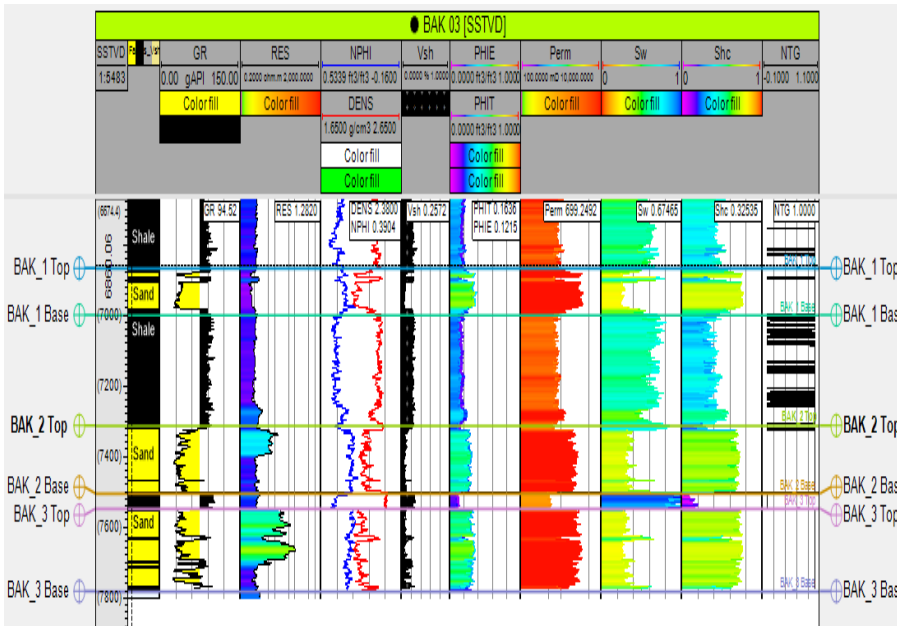


Fig. 10: Well BAK 03 showing correlated Petrophysical parameters.

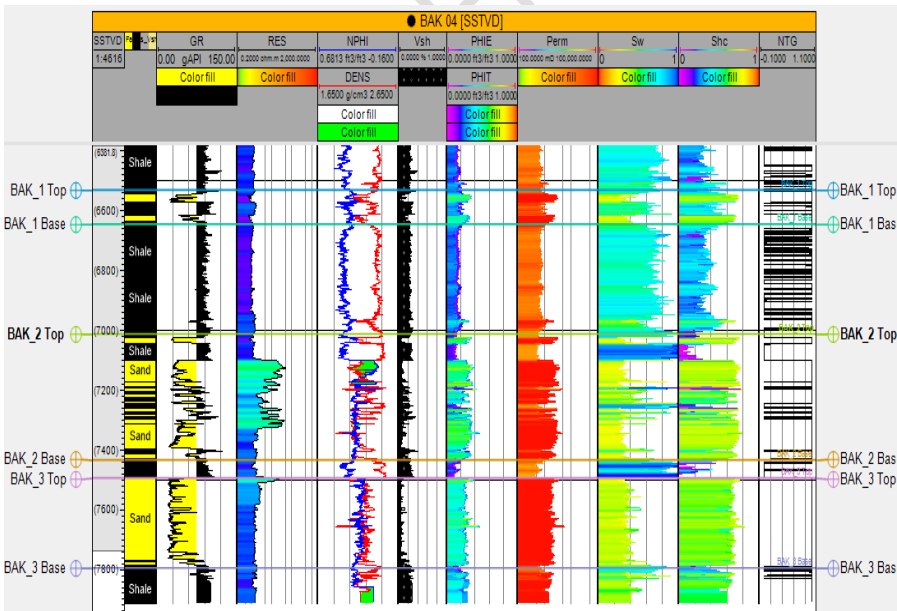


Fig. 11: Well BAK 04 showing correlated Petrophysical parameters.

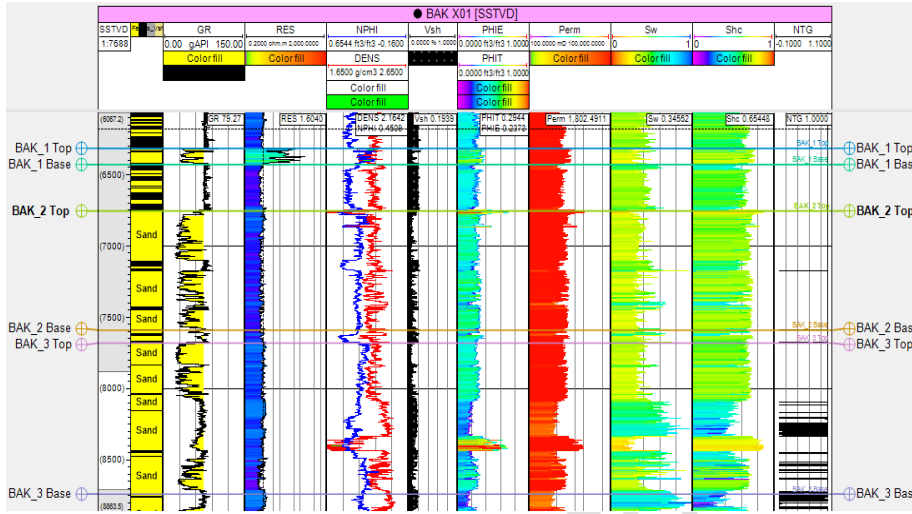


Fig. 12: Well BAK X01 showing correlated Petrophysical parameters.

Table 2: Results of Petrophysical evaluation of delineated reservoir units in the five wells in BAK Field.

Well	Reservoir Sand	Top (ft)	Base (ft)	Gross Thickness (ft)	Shale Volume (%)	Shale Volume (ft)	Net Sand (ft)	Net-to-Gross (%)	Total Porosity (%)	Effective Porosity (%)	Water Saturation (%)	Permeability (mD)	Hydrocarbon Saturation (%)	Fluid type	STOIP (stb)
BAK 01	BAK_1	5981.54	6070.82	89.28	17.5	15.62	73.66	83	36	32	31	3489.86	69	Oil + water	76466.8201
	BAK_2	6349.15	7620	1270.85	13	165.21	1105.64	87	31	28	40	3244.50	60	Oil + water	873350.6718
	BAK_3	7924.59	8465.49	540.9	13	70.32	470.58	87	25	22	45	1806.47	55	Oil + water	267724.0804
BAK 02	BAK_1	6652.88	6797.38	144.5	16	23.12	121.38	84	28	24	48	2436.85	52	Oil + water	71224.19503
	BAK_2	7144.17	7413.89	269.72	15	40.46	229.26	85	28	24	42	1234.21	58	Oil + water	150050.395
	BAK_3	7490.95	8160.45	669.5	14.24	95.34	574.16	86	25	23	56	1960.24	44	Oil + water	273200.6305
BAK 03	BAK_1	6872.12	7001.76	129.64	16.39	21.25	108.39	84	25	21	49	2096.54	51	Oil + water	54582.38993
	BAK_2	7314.68	7506.9	192.22	7.025	13.50	178.72	93	23	21	47	1677.57	53	Oil + water	93524.57758
	BAK_3	7551.6	7784.06	232.46	15.9	36.96	195.50	84	28	28	40	1903.16	60	Oil + water	154425.6159
BAK 04	BAK_1	6529.88	6643.2	113.32	19.41	22.00	91.32	81	26	22	59	1758.37	41	Oil + water	38731.12307
	BAK_2	7010.37	7431.93	421.56	19.77	83.34	338.22	80	25	23	58	1611.56	42	Oil + water	153616.9526
	BAK_3	7495.39	7794.57	299.18	13.86	41.47	257.71	86	27	25	44	3246.73	56	Oil + water	169641.1829
BAK X01	BAK_1	6310.02	6427.9	117.88	15.14	17.85	100.03	85	28	25	39	1616.17	61	Oil + water	71726.36623
	BAK_2	6749.38	7585.25	835.87	14.47	120.95	714.92	86	31	29	57	3125.86	43	Oil + water	419169.3266
	BAK_3	7681.7	8737.25	1055.55	13.21	139.44	916.11	87	36	31	56	4886.79	44	Oil + water	587528.1773

Table 3: Estimated average values of the Petrophysical properties of the reservoirs for the five wells.

Reservoirs	Gross Thickness (ft)	Shale Volume (%)	Shale Volume (ft)	Net Sand (ft)	Net to Gross (%)	Total Porosity (%)	Effective Porosity (%)	Water Saturation (%)	Permeability (mD)	Hydrocarbon Saturation (%)	STOOIP (stb)
BAK_1	118.924	16.888	19.96689	98.95711	83.112	28.636	24.812	45.19	2279.558	54.81	62546.18
BAK_2	598.044	13.853	84.69295	513.351	86.147	27.808	24.928	48.684	2178.738	51.316	337942.4
BAK_3	559.518	14.042	76.70389	482.8141	85.958	28.378	25.826	48.1481	2760.678	51.8519	290503.9

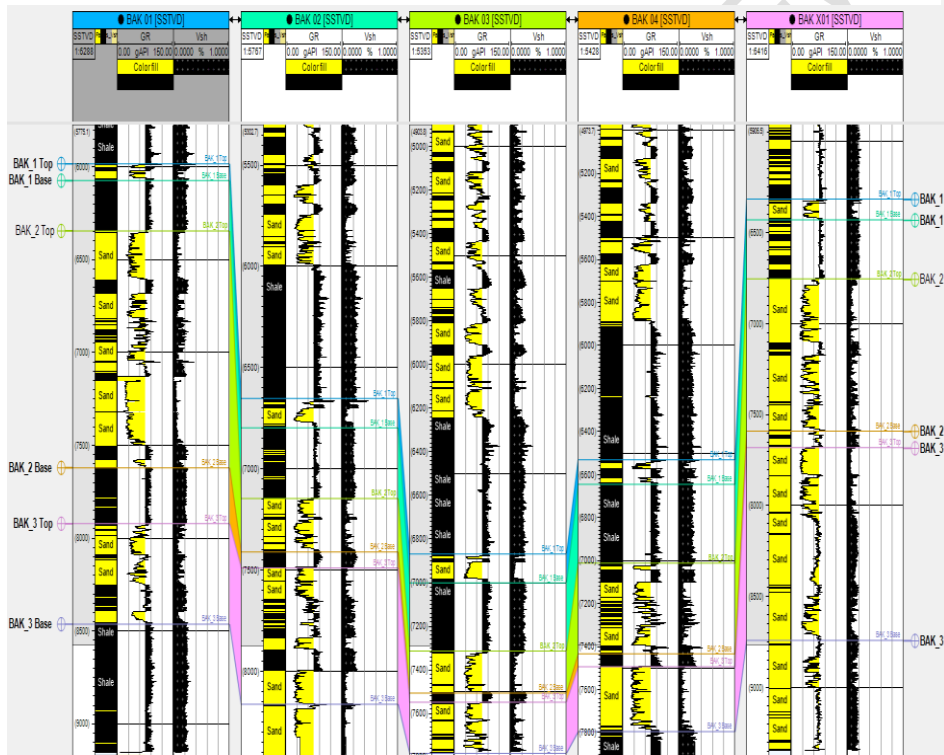


Figure 13: Well correlations showing the distribution of the volume of shale

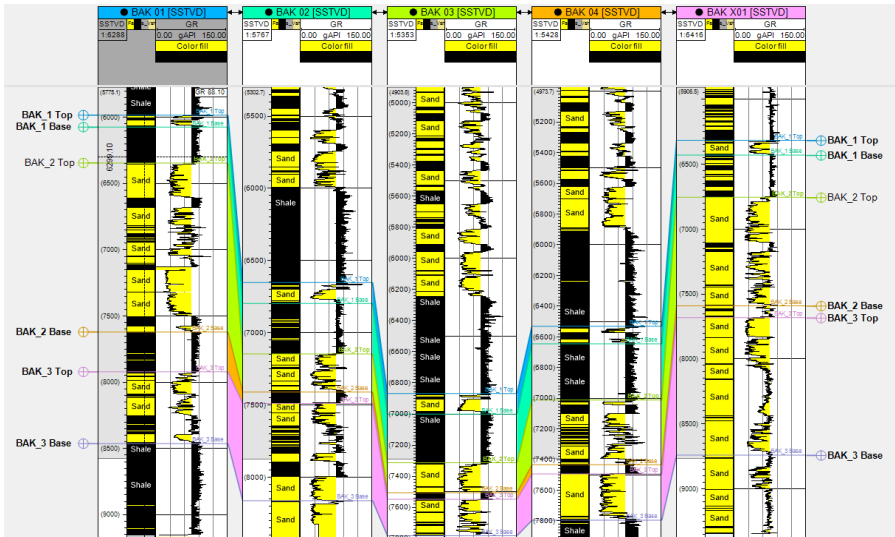


Figure 14: Top and base of reservoir intervals identified and correlated across five wells.

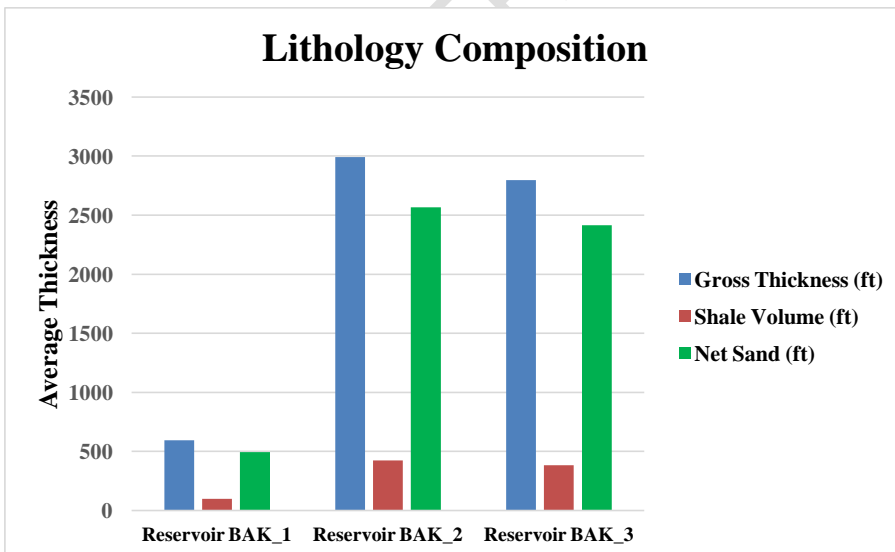


Figure 15: Average gross thickness, shale volume thickness and net sand thickness for the three reservoir intervals

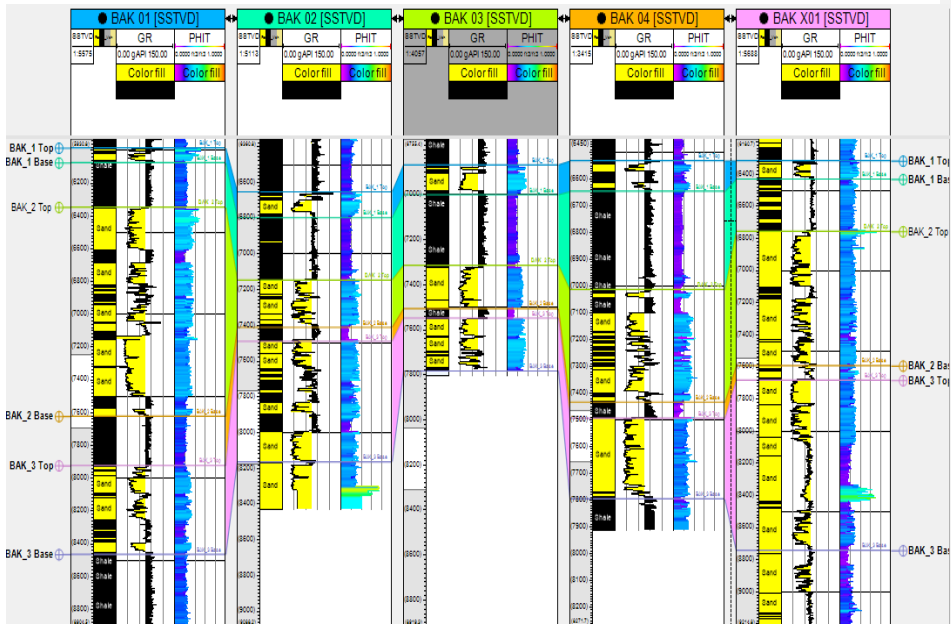


Figure 16: Total porosity estimated for the three reservoir intervals across all five wells.

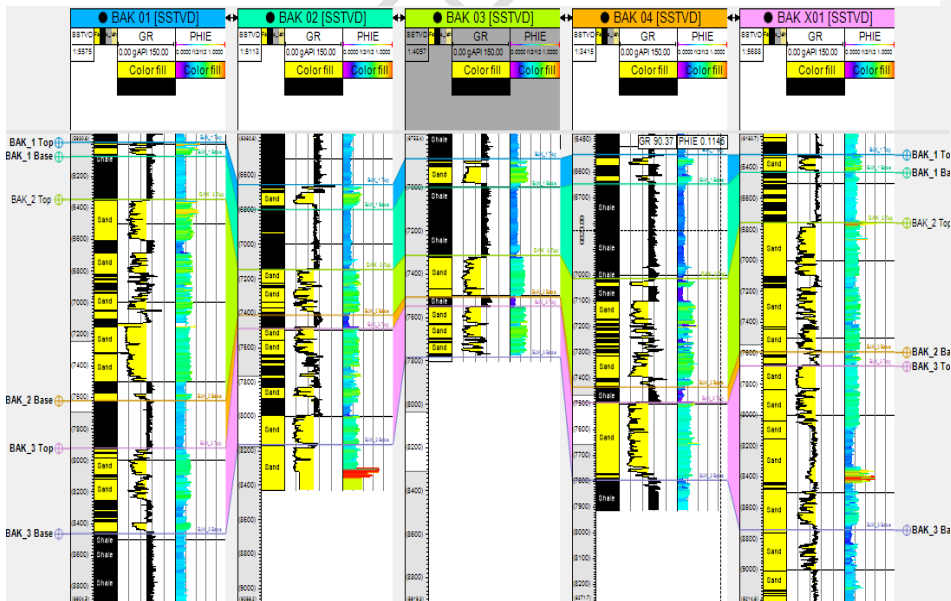


Figure 17: Effective porosity estimated for the three reservoir intervals across all five wells.

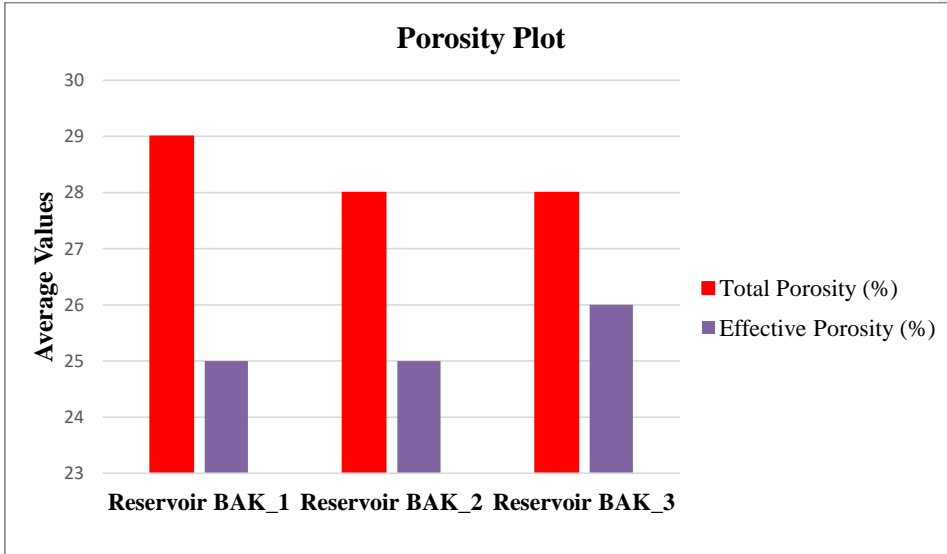


Figure 18: Average and effective porosity, calculated for the three reservoir intervals.

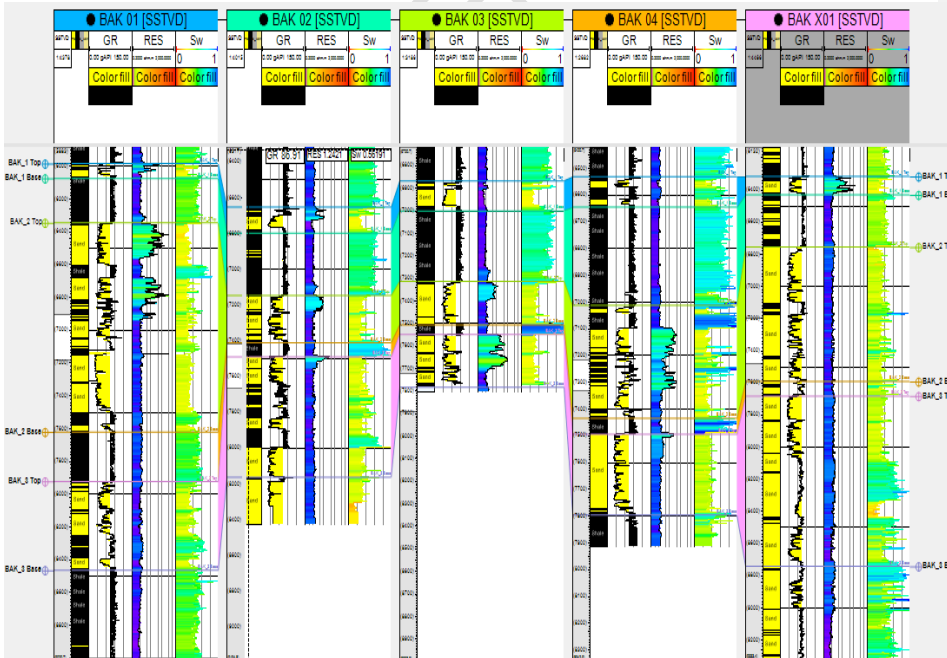


Figure 19: Water saturation calculated for the three reservoir intervals and correlated across all five wells.

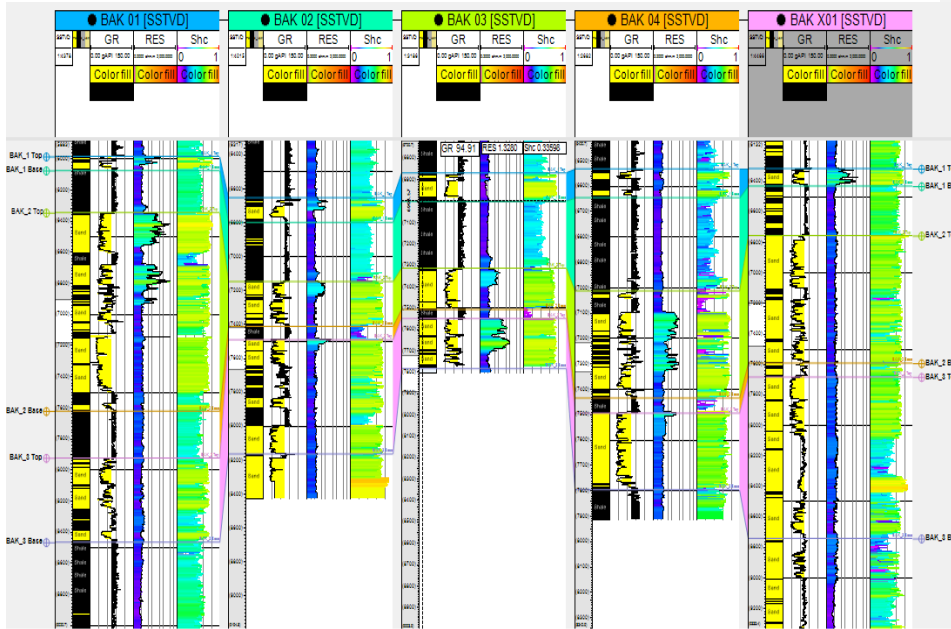
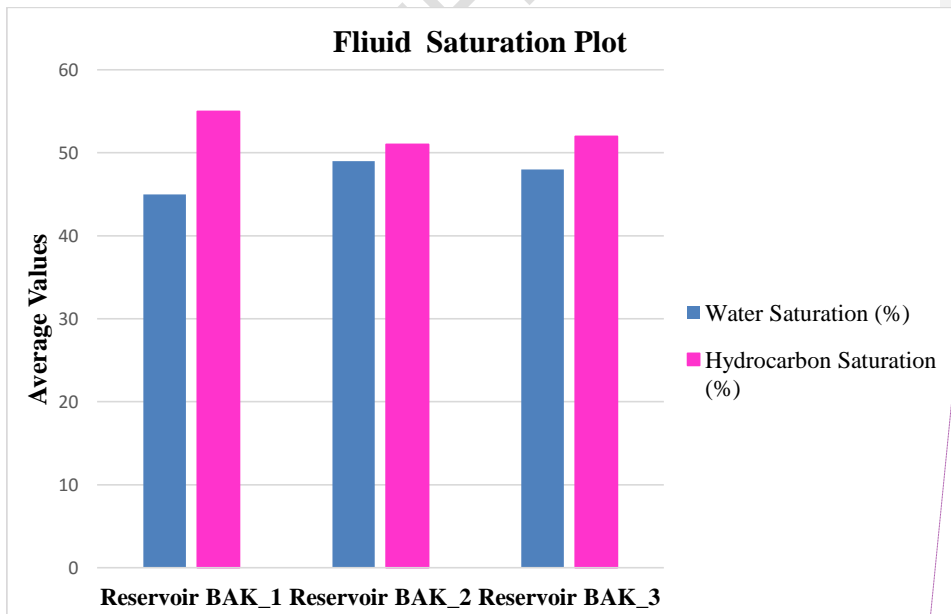


Figure 20: Hydrocarbon saturation calculated for the three reservoir intervals and correlated across all five wells.



Comment [R4]: Fluid Saturation Plot

Figure 21: Fluid saturation plots revealing water and hydrocarbon saturations estimated for the three reservoir intervals.

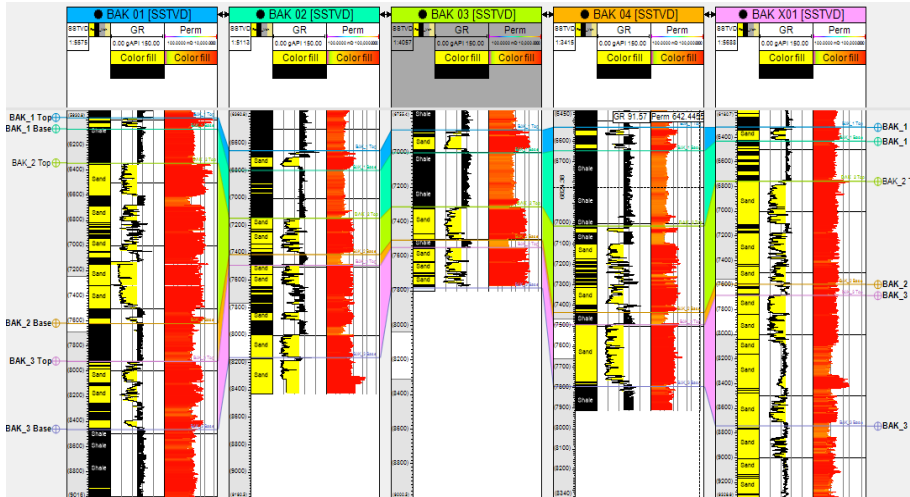


Figure 22: Permeability values estimated for the three reservoir intervals and correlated across all five wells.

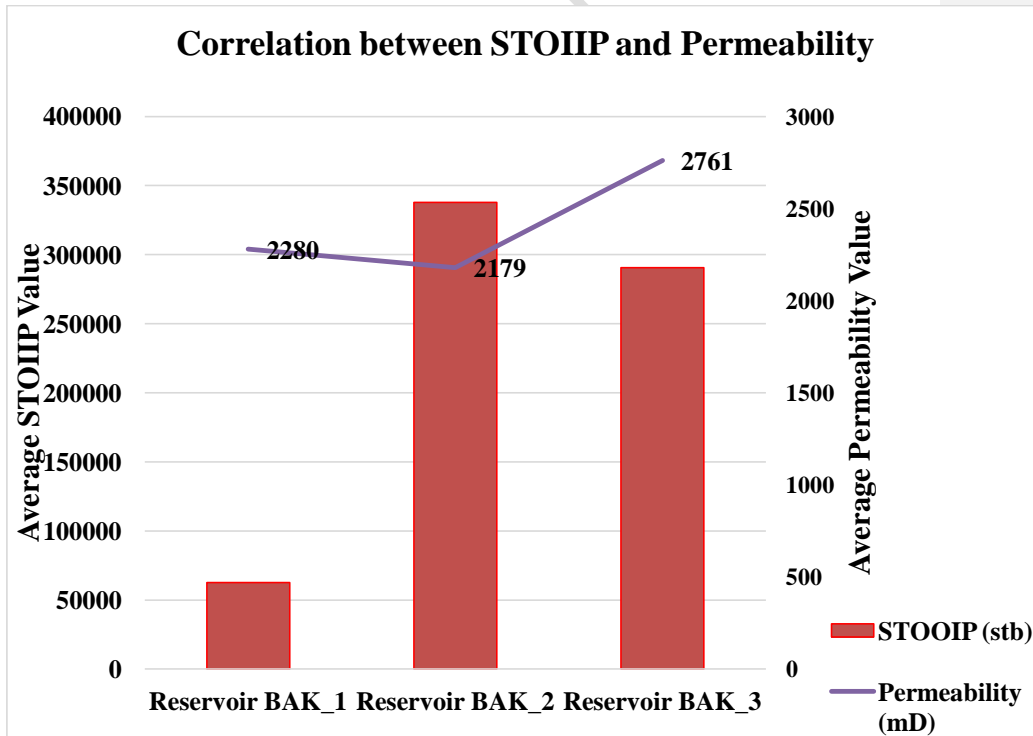


Figure 23: Correlation plot of average STOIP against average permeability

3.2. DISCUSSION

In the reservoir study, a petrophysical analysis was performed to evaluate the reservoir petrophysical properties for the three reservoirs identified and delineated for the field of study, namely BAK_1, BAK_2, BAK_3 reservoirs respectively. On average, the gross thickness of reservoir BAK_1 was found to be 118.92 ft, 598.04 ft for reservoir BAK_2 and 559.52 ft for reservoir BAK_3 respectively within the five wells used for the study (Figures 8, 9, 10, 11, 12, 13). The average gross thickness of the reservoirs shows that reservoir BAK_2 has the highest thickness while reservoir BAK_01 has the lowest thickness. These results show that the reservoir sands are of sufficient thickness to accumulate hydrocarbons in economic quantities. The Shale volume thickness determined was 19.97 ft in reservoir BAK_1, 84.69 ft in reservoir BAK_2 and 76.70 ft in reservoir BAK_3 (Table 2). This result shows that about 19.97 ft of the average gross thickness in reservoir BAK_1 is occupied by shale, 84.69 ft of the average gross thickness of reservoir BAK_2 is occupied by shale while 76.70 ft of the average gross thickness of reservoir BAK_3 is shaly. The average net to gross ratio obtained for reservoirs BAK_1, BAK_2 and BAK_3 were 83%, 86%, and 86% respectively (Table 3). These results show that on average, over 85% of the entire gross thickness of the field reservoirs (BAK_1, BAK_2 and BAK_3) can be produced if they contain hydrocarbons (Figure 13 and 14). The bar chart analysis shows that field has good thickness for hydrocarbon accumulation (Figure 15). The average total and effective porosity for reservoir BAK_1 was estimated to be 29% and 25%, while reservoir BAK_2 has 28% and 25% as total and effective porosity, the average total and effective porosity for reservoir BAK_3 was found to be 28% and 25% (Figure 16 and 17). According to Rider (1986) classification, porosity measurements between 10%-20% are considered as **good**, porosity values between 20%-30% are classified as **very good**, while values above 30% are classified as **excellent**. Based on this classification scheme, which is globally accepted for porosity classification, the total and effective porosities obtained for reservoir BAK_1, BAK_2 and BAK_3 are classified as very good reservoirs (Figure 18). The average water and hydrocarbon saturation values for reservoir are BAK_1, BAK_2, BAK_3 was 45% and 49% for BAK_1, 48% and 55% for BAK_2, 51% and 52% for BAK_3 respectively (Figure 19 and 20). These results show that reservoir BAK_1 has the highest hydrocarbon saturation while reservoir BAK_3 has the least hydrocarbon saturation measurement (Table 3), the results shows that all the identified reservoirs within the field have hydrocarbon saturation above 50%, which means they are good hydrocarbon bearing reservoirs (Figure 21). On average, permeability values estimated for the reservoir units were 2279.56mD, 2178.74mD and 2760.68mD in reservoirs BAK_1, BAK_2 and BAK_3 respectively (Table 3 and Figure 22). Rider (1986) classification of reservoir quality based on permeability values are classified as follows; k values below 10mD considered as **poor to fair**, k values between 10-50 mD classified as **moderate**, k values between 50-250 mD are classified as **good**, k values between 250-1000 mD are classified as **very good**, and k values above 1000 mD are classified as **excellent**. Based on this classification scheme, reservoirs BAK_1, BAK_2 and BAK_3 can be classified within the ranges of excellent reservoirs because they have average permeability values above 1000mD respectively. These results show that all the reservoirs in the field have excellent permeability values which are necessary requirements for hydrocarbon flow and production in economic quantities. A correlation of the permeability with the estimated STOOIP of the different reservoir units shows the effect of permeability on the productivity ability of the field (Figure 23). The result shows that the field is economically viable for hydrocarbon exploitation.

4. CONCLUSION

The use of well logs evaluation, well log correlation and petrophysical analysis was carried out to evaluate petrophysical properties in the field of study. In the reservoir delineation, three

Comment [R5]: Please provide interpretation for your correlation, is it high, average or low? Do we have a positive or negative value? Also provide implication for the description of your correlation based on Figure 23.

lithologic sand reservoirs were identified using gamma ray, resistivity and the cross plot of neutron and density logs. Three reservoirs identified and correlated for the five wells (BAK 01, BAK 02, BAK 03, BAK 04, and BAK X01) using gamma ray, gives the estimated average thickness for the three reservoirs BAK_1, BAK_2, and BAK_3 as 118.92 ft, 598.04 ft and 559.52 ft respectively. The petrophysical analysis helps to estimate the total porosity, permeability, water saturation, shale volume, effective porosity and hydrocarbon saturation to quantify the extent of producibility of the three reservoirs. The reservoir study evaluated and obtained the following petrophysical parameters for the field as follows; the average effective porosity as 25%, total porosity estimated to be 28%, the average shale volume of 45%, average water saturation of 47%, average hydrocarbon saturation of 53%, average permeability of 2406.325mD, and an average reserve estimate of 23 MMstb (STOOIP). From the reservoir study of the field using the results of petrophysical analysis which reveals a low shale volume, high effective and total porosities (good porosity), low water saturation, and excellent permeability, we can conclude that the petrophysical analysis has shown that the three reservoirs units identified were of good reservoir quantities as the. Thus, the reservoir sand body can be said to be a good reservoir for hydrocarbon exploitation and production.

Comment [R6]: These statements are more of a findings / the conclusion is a general statement that answers your main problem, that is to evaluate the petrophysical properties of....

CONSENT (WHERE EVER APPLICABLE)

All authors declare that written informed consent was obtained from the patient (or other approved parties) for publication of this case report and accompanying images. A copy of the written consent is available for review by the Editorial office/Chief Editor/Editorial Board members of this journal.

COMPETING INTERESTS DISCLAIMER:

Authors have declared that no competing interests exist. The products used for this research are commonly and predominantly use products in our area of research and country. There is absolutely no conflict of interest between the authors and producers of the products because we do not intend to use these products as an avenue for any litigation but for the advancement of knowledge. Also, the research was not funded by the producing company rather it was funded by personal efforts of the authors.

REFERENCES

- [1]. **Adiela UP, Omoboriowo AO.** Depositional Environment and Petrophysical Studies of Ako Reservoir Sands, Niger Delta. *International Journal of Scientific Engineering and Science.* **2018;** 2(3):5-10.
- [2]. **Evamy BD, Haremboure J, Kamerling P, Knaap WA, Molloy FA, Rowlands PH.** Hydrocarbon habitat of Tertiary Niger Delta. *American Association of Petroleum Geologists (AAPG) Bulletin.* **1978;** 62:277-298.
- [3]. **Adiela UP, Itiowe K, Emudianughe J.** Seismic And Petrophysical Attributes of Reservoirs in "Ebi" Oil Field, Niger Delta. *International Journal of Science Inventions Today.* **2016;** 5(3):273-282.
- [4]. **Obiekezie TN, Basseyy EE.** Petrophysical analysis and volumetric estimation of Otu field, Niger Delta Nigeria, using 3D seismic and well log data. *Physical Science International Journal.* **2015;** 6(1):54-65.
- [5]. **Cannon AG.** Petrophysics: A practical Guide, Wiley Blackwell. **2015;** 1- 224
- [6]. **Ekine AS, Iyabe P.** Petrophysical characterization of the Kwale field reservoir sands (OML 60) from wire-line logs, Niger Delta, Nigeria. *Journal of Applied Science and Environmental Management.* **2009;** 13(4): 81 – 85.

- [7]. **Avbovbo AA.** Tertiary lithostratigraphy of Niger Delta. *American Association of Petroleum Geologists Bulletin, Tulsa, Oklahoma.* **1978**; 96–200.
- [8]. **Klett TR, Ahlbrat TS, Schmoker JW, Dolton JL.** Ranking of the world's oil & gas provinces by known petroleum volumes. *U.S. Geological Survey Open-file Report CD-ROM.* **1997**; 97 - 463.
- [9]. **Doust H, Omatsola E. (1990).** Niger Delta. In: Edwards, J. D., and Santogrossi, P.A., eds., Divergent/passive Margin Basins. *American Association of Petroleum Geologists (AAPG) Memoir.* 1990; 48:239-248.
- [10]. **Weber KJ.** Sedimentological aspects of oil fields in Niger Delta. *Geologize en Mingbouw.* **1971**; 50: 559 - 576.
- [11]. **Hospers J.** Gravity field & structure of the Niger Delta, Nigeria, West Africa. *Geological Society of American (AAPG) Bulletin.* **1965**; 76:407-422.
- [12]. **Merki P.** Structural Geology of the Cenozoic Niger Delta. Africa Geology, University of Ibadan Press. T.F.J. **1970**; 1 - 268
- [13]. **Ekweozor CM, Daukoru EM. (1994).** Northern delta Depobelt portion of the Akata – Agbada Petroleum system, Niger Delta: In Magoon, L.B. and Dow, W.G. (Eds). The petroleum system from source to trap. *American Association of Petroleum Geologists (AAPG)Memoir.* **1994**; 4(6):599 – 613.
- [14]. **Orife JM, Avbovbo AA.** Stratigraphic and unconformity traps in the Niger Delta. *American Association of Petroleum Geologists (AAPG) Bulletin.* **1982**; 65:251-265.
- [15]. **Corredor F, Shaw JH, Bilotti F.** Structural styles in the deep-water fold and thrust belts of the Niger Delta. *American Association of Petroleum Geologists (AAPG) Bulletin.* **2005**; 89:753 – 780.
- [16]. **Short KC, Stauble AJ. (1967).** Outline of geology of Niger Delta. *American Association of Petroleum Geologists (AAPG) Bulletin.* **1967**; 51:761 – 779.
- [17]. **Weber KJ, Daukoru E.** Petroleum Geology of the Niger Delta. *Ninth World Petroleum Congress Proceedings.* **1975**; 2:209 – 221.
- [18]. **Weber KJ.** Hydrocarbon distribution patterns in Nigerian growth fault structures controlled by structural style & Stratigraphy. *Journal of Petroleum Science and Engineering.* **1987**; 1:91- 104.
- [19]. **Nwachukwu JI, Chukwurah PI.** Organic Matter of Agbada Formation, Niger Delta, Nigeria. *American Association of Petroleum Geologist Bulletin.* **1986**; 70:48-55.
- [20]. **Stacher P.** Present understanding of the Niger delta hydrocarbon habitat: Geology of Deltas. *AA Balkema, Rotterdam.* **1995**; 257–267.
- [21]. **Ejedawe JE, Coker SJL, Lambert-Aikhionbare DO, Alofe KB, Adoh, FO.** Evolution of Oil Generating Window and Gas. *American Association of Petroleum Geologist (AAPG)Bulletin.* **1984**; 68:1744-1751.
- [22]. **Beka FT, Oti MN.** The distal offshore Niger Delta: frontier prospects of a mature petroleum province, in, Oti, M.N., & Postma, G., (eds), Geology of Deltas. *Rotterdam, A.A. Balkema,* **1995**; 237-241.
- [23]. **Tissot BP.** Petroleum Formation and Occurrence. *Berlin, Springer-Verlag.* **1954**; 1-518.
- [24]. **Adeoti L, Ayolabi EA, James PL.** An Integrated Approach to Volume of Shale Analysis: Niger Delta Example, Orire Field. *World Applied Sciences Journal.* **2009**; 7(4): 448-452.
- [25]. **Adiela UP.** Reservoir and Petrophysical Studies of Kora Well Onshore, Niger Delta Field, Nigeria. *International Journal of Innovative Research in Science, Engineering and Technology.* **2018**; 7(11).
- [26]. **Archie GE.** The Electrical Resistivity Log as an aid in determining some reservoir characteristics. *Journal of Petroleum Technology.* **1942**; 5:54-62.
- [27]. **Burke K.** Longshore drift, submarine canyons, & submarine fans in Development of Niger Delta. *American Association of Petroleum Geologists (AAPG) Bulletin.* **1972**; 56:1975-1983.

- [28]. **Edohor EH, Ayomide BO.** Petrophysical Evaluation of H-field, Onshore Niger Delta Sedimentary Basin, Nigeria. *Asian Journal of Geological Research.* **2020**; 3(2): 1-16.
- [29]. **Eke IJ.** Petrophysical Evaluation of Hydrocarbon Bearing Sands in "MANIN" Marginal Field, Onshore Niger Delta. *Journal of Applied Geology and Geophysics (IOSR-JAGG).* **2020**; 8(3): 2.
- [30]. **Ekweozor CM, Okoye NV.** Petroleum source-bed evaluation of Tertiary Niger Delta. *American Association of Petroleum Geologists (AAPG) Bulletin.* **1980**; 64:1251-1259.
- [31]. **Eze MO, Mode AW, Anyiam AO.** Recognition and Evaluation of Low Resistivity Pay-Zones: A Case Study of "Amo-Field" in the Tertiary Niger Delta Basin, Nigeria. *The Pacific Journal of Science and Technology.* **2016**; 17(1): 21-32
- [32]. **Hilchie DW.** Applied Openhole Log Interpretation. D.W. Hilchie, Inc.: Golden, CO. **1978**; 1-161.
- [33]. **Hunt JM.** Generation & migration of petroleum from abnormally pressured fluid compartments. *American Association of Petroleum Geologists Bulletin.* **1990**; 74:1-12.
- [34]. **Ideozu UR, Ehilegbu MN, Okujagu DC.** Petrophysical Analysis of Egbu Field, Offshore Niger Delta, Nigeria, Using Well Log, Core Data and Pearson's Matrices. *Journal of Mining and Geology.* **2020**; 56(2):329 - 346.
- [35]. **Kulke H.** Nigeria, in, Kulke, H., ed., Regional Petroleum Geology of the World. Part II. *frica, America, Australia and Antarctica: Berlin, GebrüderBorntraeger, Germany.* **1995**; 143-172.
- [36]. **Larionov V.** Borehole Radiometry: Moscow, U.S.S.R., Nedra. **1969**; 34-45.
- [37]. **Ogidi AO, Ekhalialu OM, Okon EE.** Petrophysical Evaluation of Otebe Field, Onshore Niger Delta, Nigeria. *International Journal of Research and Innovation in Applied Science.* **2018**; 3(11).
- [38]. **Oyeyemi KD, Olowokere MT, Aizebeokha AP.** Hydrocarbon resource evaluation using combined petrophysical analysis and seismically derived reservoir characterization, offshore Niger Delta. *Journal of Petroleum Exploration and Production Technology.* **2017**; 3:35-48
- [39]. **Paul SS, Okwueze EE, Udo KI.** Petrophysical Analysis of Well Logs for the Estimation of Oil Reserves in Southern Niger Delta. *International Journal of Advanced Geosciences.* **2018**; 6(1):140-145.
- [40]. **Peters EJ.** Petrophysics. *Department of Petroleum and Geosystems Engineering, The University of Texas at Austin.* **2001**; 1-184
- [41]. **Saleh MB, Babajika MI, Terrang SU.** Geology and Petrophysical Analysis of Oredo Oil Field in Niger Delta Basin, Southern Nigeria. *International Journal of Science and Research.* **2018**; 301 - 306.
- [42]. **Sanuade OA, Akanji AO, Olajojo AA, Oyeyemi KD.** Seismic interpretation and petrophysical evaluation of SH field, Niger Delta. *Journal of Petroleum Exploration and Production Technology.* **2017**; 2:1-21
- [43]. **Schlumberger.** Log interpretation, principles, and application. *Schlumberger wireline and testing. Texas, USA.* **1985**; 21-89.
- [44]. **Victor CN, Ezenwaka KC, Ede TA.** Evaluation of hydrocarbon reserves using integrated petrophysical analysis and seismic interpretation: A case study of TIM field at southwestern offshore Niger Delta oil Province, Nigeria. *Egyptian Journal of Petroleum.* **2019**; 28:273 -280.